Silylated Coumarin Dyes in Sol−Gel Hosts. 2. Photostability and Sol−Gel Processing

T. Suratwala,* Z. Gardlund, K. Davidson, and D. R. Uhlmann

Department of Materials Science and Engineering, Arizona Materials Laboratory, University of Arizona, Tucson, Arizona 85712

J. Watson, S. Bonilla, and N. Peyghambarian

Optical Sciences Center, University of Arizona, Tucson, Arizona 85721

Received May 8, 1997. Revised Manuscript Received September 25, 1997[⊗]

The photostability characteristics of numerous silylated coumarin dyes within SiO_2 xerogels and SiO_2:PDMS Polyceram films, and of neat silylated coumarin dye films have been determined and related to the sol−gel processing conditions and host composition. FTIR spectroscopy was used to monitor the hydrolysis reaction rates of the silylated dyes and other Si−alkoxide precursors. The silylated dyes had varying reaction rates depending on the degree of functionality and the linkage between the alkoxide and the dye. Matching the reaction rates between TMOS and the silylated dye was accomplished by prehydrolysis of the silylated dye. The photostability of the dyes in the xerogels was measured by monitoring the drop in fluorescence intensity upon pumping with a N_2 laser and also by monitoring the drop in dye absorption upon irradiating the films with a UV lamp. At optimized prehydrolysis times, a silylated coumarin dye (derCoum) within a SiO_2 xerogel host demonstrated a 3-fold improvement in long-term photostability compared to its unsilylated counterpart. The use of a silylated dye results in covalently bonding the dye to the host matrix, increasing the probability that the dye will be caged and inhibiting dynamic processes which can lead to photodegradation. CP-MAS ^{29}Si NMR data for a derCoum xerogel confirmed that a large degree of dye bonding occurred. The addition of PDMS to the basic SiO_2 xerogel host composition had little effect on the photostability of the dye. The neat dye films showed improved fluorescence photostability with increase in hydrolysis time. These films showed poor photostability upon exposure to UV lamp degradation due to lower thermal degradation resistance and/or thermal conductivity compared to the SiO_2 xerogel films.

1. Introduction

Solid hosts containing laser dyes hold much promise as the gain media for visible, tunable solid-state lasers. A solid-state dye laser would be useful for numerous low- and high-power applications in areas such as medicine and defense.[1,2] The lack of photostability has been the major factor that has limited their commercial use.

The lack of photostability (bleaching) of a fluorescent dye represents the permanent decline in the fluorescence output upon optical pumping, typically reflecting the chemical modification of the molecule. An excited dye molecule can return to the ground state by a number of pathways, either intramolecular or intermolecular, as illustrated schematically in Figure 1.[3] Intramolecular interactions include photophysical processes such as radiative (k_f) and nonradiative (k_i, k_{ic}) transitions and photochemical processes as isomerization reactions. Intermolecular interactions can result in photochemical reactions, deactivation processes, and quenching processes. The two major photochemical reactions, oxidation and dimerization reactions, cause destruction of the original dye molecule and permanent drop in the fluorescence output.

Molecular oxygen (O_2) plays a special role in organic photochemistry, because it has an unusual triplet ground state and a very low excited singlet state. O_2 is a very good triplet-state quencher, and in its excited singlet state, it is reactive toward many organic compounds. The formation of singlet oxygen is illustrated by the following reaction:

$$^3A^* + {}^3O_2 \rightarrow {}^1A + {}^1O_2^*$$

where oxygen quenches the triplet state of an organic molecule (A). The 4-methyl groups in many coumarin dyes are particularly prone to oxidation.[4−10] For ex-

[⊗] Abstract published in *Advance ACS Abstracts,* December 1, 1997.

(1) Fitzpatrick, R. *Opt. Photonics News* **1995**, *6*, 23−31.
(2) Aldag, H. *Vis. UV Lasers* **1994**, *SPIE 2115*, 184−189.
(3) Coyle, J. *Introduction to Organic Photochemistry*; John Wiley & Sons: Chichester, 1986.
(4) Winters, B.; Juneau, R.; Schulman, S. *Appl. Phys. Lett.* **1972**, *25*, 723−724.
(5) Kalmykova, E.; Kuznetsova, N.; Kaliya, O. *Zh. Obsh. Khim.* **1990**, *60*, 946−951.

S0897-4756(97)00340-2 CCC: $15.00 © 1998 American Chemical Society
Published on Web 01/19/1998

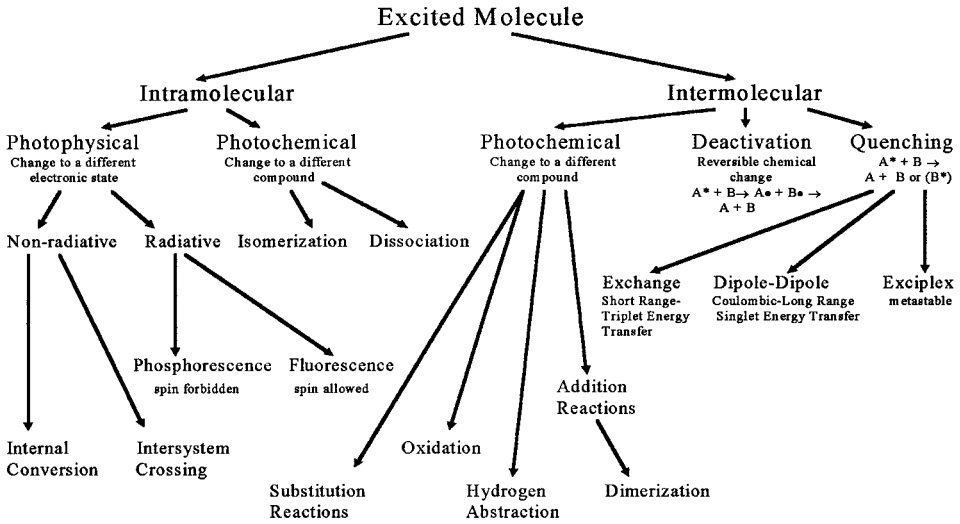

Figure 1. Intramolecular and intermolecular pathways for an excited-state organic molecule.

ample, the 4-methyl group in 7-(diethylamino)-4-methylcoumarin leads to the formation of a carboxylic acid upon photooxidation.[4,5] Other addition reactions can occur as well. Dimerization reactions are common with many dye molecules including coumarin dyes.[11,12]

In addition to photooxidation and photodimerization, dye degradation can occur thermally. With high-intensity optical pumping, absorption by the host matrix (inner filter effects) and by the dye can produce sufficient heat for thermal oxidation. Thermal oxidation can occur from the formation of an allyl radical by the abstraction of allylic hydrogen by the oxygen.[13]

With the mechanisms of photodegradation discussed above, improvement in photostability can be achieved by caging or isolating the dye, which reduces its interaction with other species (e.g., oxygen, other dye molecules). Caging a laser dye within a silica matrix has shown improved photostability with respect to solvent hosts.[14−16] Silylated dyes (also referred to as grafted or functionalized dyes) are organic molecules that have been chemically altered to provide alkoxysilane functionality. This allows the dye molecule to participate in the hydrolysis and condensation reactions during sol−gel processing of the host and allows the active molecule to bond covalently to the host matrix. Covalent dye attachment will inherently prevent the dye from having translational motion within the pores of the silica matrix. This should decrease the number of dynamic interactions producing photodegradation. Also, covalently bonding the dye as opposed to simple dissolution of the dye within the matrix increases the probability that the dye will be completely caged by the silica matrix, reducing the extent to which impurities or nonbonded dyes will migrate to and interact with the caged molecules. The increased probability of caging stems from the fact that the dye already has a portion of itself protected by the alkoxysilane group, and the silane is very likely to interact with the silica matrix to create a more complete cage. In concurrent work, it was concluded that only a small percentage of an unsilylated dye within a sol−gel host was caged.[17] The use of silylated dyes with a sol−gel matrix should provide improved photostability compared with their unsilylated counterparts due to the increased probability of dye caging.

In previous publications, we have illustrated the synthesis and incorporation of numerous silylated coumarin dyes within sol−gel hosts. The use of silylated laser dyes resulted in (1) improved solubility of the silylated dye with respect to its unsilylated counterpart, allowing for higher concentrations of active molecules within a sol−gel matrix;[18] (2) higher fluorescence efficiency, attributed to the greater rigidity and isolation of the silylated dye within its host;[18] (3) improved chemical stability, associated with the inability to leach the dye from the host;[18] and (4) control of dye/matrix interactions affecting optical spectra.[19]

With the advantages listed above, there is a need to examine in more detail the photostability characteristics of silylated dyes incorporated within sol−gel matrixes. In the present paper, the photostability of various silylated coumarin dyes within various sol−gel derived hosts are examined in detail. The photostability characteristics are related to the dye structure, host composition, and sol−gel processing parameters, most notably the reaction kinetics.

(6) Priyadarsini, K.; Kunjappu, J.; Moorthy, P. *Indian J. Chem.* **1987**, *26A*, 899−901.
(7) JonesII, G.; Bergmark, W.; Jackson, W. *Opt. Commun.* **1984**, *50*, 320−324.
(8) Fletcher, A. *Appl. Phys.* **1977**, *14*, 295−302.
(9) Reynolds, G.; Drexhage, K. *Opt. Commun.* **1975**, *13*, 222−225.
(10) Schimitschek, E.; Trias, J.; Hammond, P.; Henry, R.; Atkins, R. *Opt. Commun.* **1976**, *16*, 313−316.
(11) Kuznetsova, N. A.; Kaliya, O. L. *Russ. Chem. Rev.* **1992**, *61*, 683−696.
(12) Muthuramu, K.; Ramamurthy, V. *Indian J. Chem.* **1984**, *23B*, 502−508.
(13) Horspool, W. *Aspects of Organic Photochemistry*; Academic Press: London, 1976.
(14) Avnir, D.; Levy, D.; Reisfeld, R. *J. Phys. Chem.* **1984**, *88*, 5956−5959.
(15) Avnir, D.; Kaufman, V.; Reisfeld, R. *J. Non-Cryst. Solids* **1985**, *74*, 395−406.
(16) McKiernan, J.; Yamanaka, S.; Dunn, B.; Zink, J. *J. Phys. Chem.* **1990**, *94*, 5652−5654.
(17) Suratwala, T.; Gardlund, Z.; Davidson, K.; Uhlmann, D. R.; Bonilla, S.; Peyghambarian, N. *J. Sol−Gel Sci. Technol.* **1997**, *8*, 953−958.
(18) Suratwala, T.; Gardlund, Z.; Boulton, J. M.; Uhlmann, D. R.; Watson, J.; Peyghambarian, N. *Sol−Gel Opt. III* **1994**, *SPIE 2288*, 310−320.
(19) Suratwala, T.; Gardlund, Z.; Davidson, K.; Uhlmann, D. R.; Watson, J.; Peyghambarian, N. *Chem. Mater.*, previous paper in this issue.

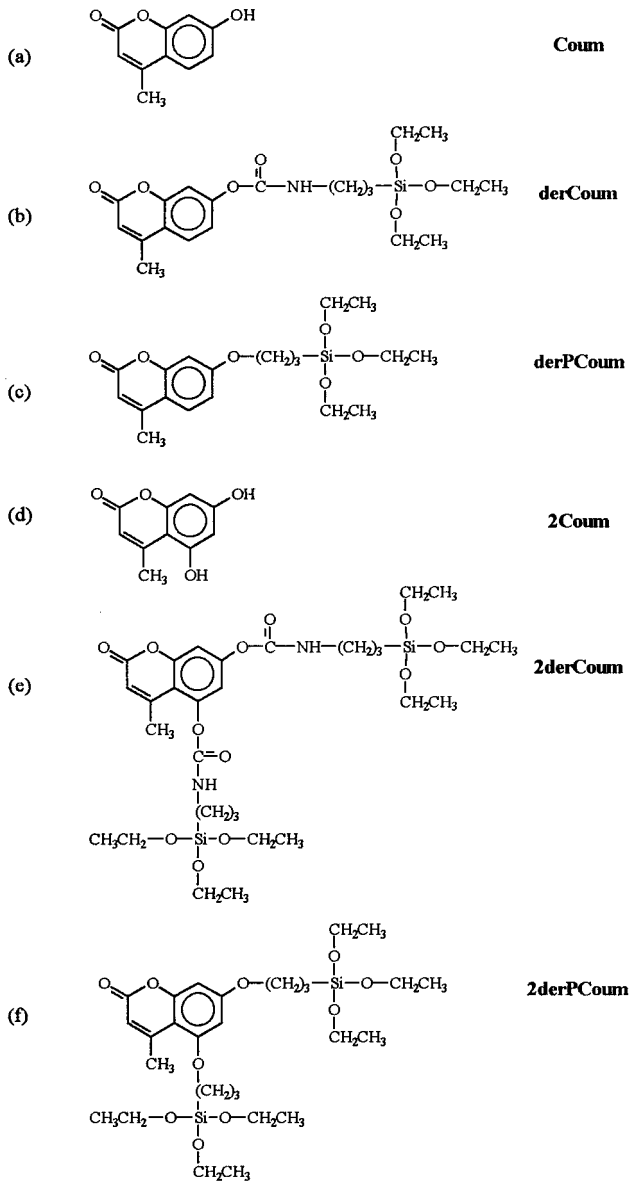

Figure 2. Structure of coumarin dyes: (a) Coum, (b) derCoum, (c) derPCoum, (d) 2Coum, (e) 2derCoum, and (f) 2derPCoum.

2. Experimental Section

Numerous coumarin dyes, 7-hydroxy-4-methylcoumarin (Coum), 7-(*N*-triethoxysilyl)-*O*-(4-methylcoumarin)urethane (derCoum), 7-(3-(triethoxysilyl)propoxy)-4-methylcoumarin (derPCoum), 5,7-bis(*N*-triethoxysilylpropyl)-O-(4-methylcoumarin)-urethane (2derCoum), and 5,7-bis-(3-(triethoxysilyl)propoxy)-4-methylcoumarin (2derPCoum), were synthesized as described elsewhere.[19] The structures of the six dyes (two unsilylated, two monofunctionalized, and two bifunctionalized) are shown in Figure 2.

Route 1: Coumarin-Doped Xerogel Films. All the coumarin dyes were separately dissolved in anhydrous THF at 11 wt %. Deionized H_2O (acidified to 0.15 M HCl) was added at H_2O:dye mole ratios of 1.5:1 for derCoum, 3:1 for 2derCoum, 1.5:1 for derPCoum, and 3:1 for 2derPCoum. No H_2O was added for the Coum:THF mixture. The solutions were refluxed for various lengths of time. Separately, tetramethoxysilane (TMOS), THF, and deionized H_2O (acidified to 0.15 M HCl) were mixed in a glass vial at a TMOS:H_2O:THF molar ratio of 1:2:5 or 1:4:5. The solution was mixed for a few minutes allowing the TMOS to hydrolyze. The dye/H_2O/THF solutions were mixed with the TMOS/H_2O/THF solutions in proper amounts, resulting in a dye:Si mole ratio of 0.05:1 ($r = 0.05$).

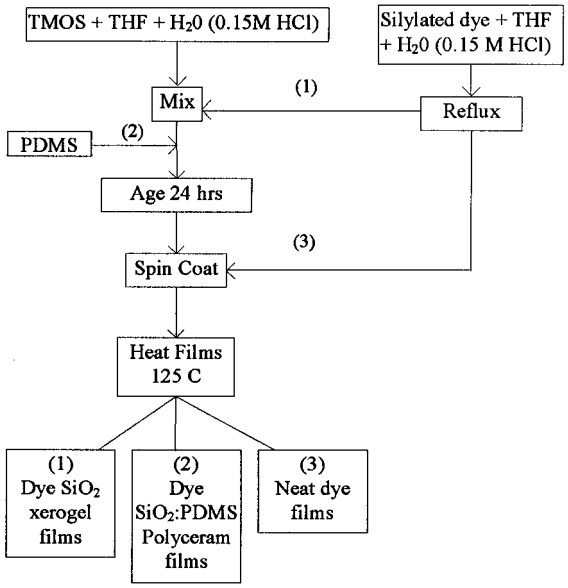

Figure 3. Preparation procedure for dye-doped xerogel films.

After aging for 24 h, the final solutions were passed through 0.2 μm filters and spin coated on precleaned microscope slides (Gold Seal) at 2000 rpm for 20 s. The films were dried at 125 C for 48 h in vacuum.

Route 2: Coumarin-Doped SiO_2:PDMS Polycerams. The SiO_2:poly(dimethylsiloxane) (PDMS) films were synthesized similarly to the route 1 xerogels except that PDMS (silanol terminated, low molecular weight (400−700) from United Chemical Technologies) was added to the dye:THF:TMOS:H_2O mixture. The final solid Polyceram contained 70 volume % PDMS.

Route 3: Neat Dye Films. It was possible to form films by hydrolysis−condensation reactions of the silylated dyes in solvent. Other silicon-containing precursors were not needed to form either a gel network or a film. The silylated dyes (11 wt % in THF) were reacted with H_2O at the same mole ratios stated above. The solutions were refluxed for various times and then spin-coated to form optically transparent films.

The dye concentrations are reported as the dye:Si mole ratio (r) and not the dye:TMOS molar ratio, where "dye" refers to the "Coum" basic ring structure. In other words, the total moles of Si results from both the TMOS and from the Si contributed from the silylated dye. For example, a $r = 1.0$ derCoum xerogel film would represent 100% derCoum composition and a $r = 0.5$ 2derCoum xerogel film would represent a 100% 2derCoum composition. For the unsilylated dye xerogel films, the dye:Si ratio is the same as the dye:TMOS ratio; while for the silylated dyes this is not the case. The dye:Si ratio is a more useful representation of the dye concentration within the sol−gel host.

The above synthetic routes are illustrated schematically in Figure 3.

FTIR Monitoring of Hydrolysis Reaction Rate. The hydrolysis reaction rate was monitored by Fourier transform infrared spectroscopy (FTIR, Perkin-Elmer 1725x). The silylated dyes were separately dissolved in anhydrous THF at 11 wt %. H_2O acidified to 0.15 M HCl was added at a 1.5:1 H_2O:silylated dye mole ratio for the monofunctionalized dyes (derCoum, derPCoum) and 3:1 for the bifunctionalized dyes (2derCoum, 2derPCoum). The same was done with tetraethoxysilane (TEOS) in THF at 2.11 mol % at a H_2O:TEOS mole ratio of 2:1. TEOS was used for the FTIR studies to serve as a control to compare with the reaction rates of the silylated dyes, because all these alkoxide precursors have ethoxide groups in their structure. All the H_2O:dye mole ratios correspond to half of the stoichiometric ratio, where the stoichiometric ratio represents one H_2O molecule for every alkoxide group on the Si−alkoxide precursor. The solutions were refluxed, and infrared spectra were taken periodically. An IR

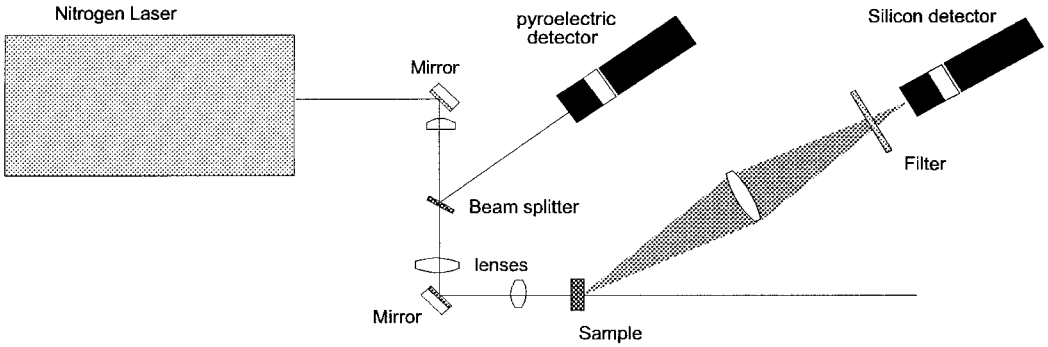

Figure 4. Schematic of the photostability measurement setup using a N_2 laser.

transparent NaCl sealed cell was used as the solution holder to prevent evaporation, allowing for quantitative analysis. Standards were run with H_2O, EtOH, TEOS, and dye separately to identify peaks. Anhydrous THF was used as the background.

Photostability Measurements. Samples (which were either the dye-doped films or the dyes in methanol (MeOH) at 10^{-4} M within quartz cuvettes) were exposed to a long-wave ultraviolet (UV) lamp (>300 nm, 8 W) located 1.5 in. away. The absorption spectra of the samples were monitored periodically with a UV−vis spectrophotometer (Perkin-Elmer Lambda 3B). The maximum absorption of the dye was normalized to the absorption before UV exposure and plotted as a function of UV exposure time. The permanent drop in the absorbance represents degradation of the dye.

Photostability was also measured by pumping the samples with a N_2 laser at 337 nm with a pulse rate of 7.7 Hz, a pulse width of 20 ns, and a fluence of 0.001 J/cm^2 (1×10^{-4} J/pulse, 0.10 cm^2 spot area). A solid angle of the fluorescence was focused onto a silicon detector (Laser Precision) after passing through a 385 nm band-pass filter to block the pump light. The fluorescence output energy per pulse was monitored as a function of number of pump pulses. A schematic of the setup is shown in Figure 4.

Dye Extraction. The xerogel films were soaked in THF at 50 °C in a closed system. The films were periodically removed and the maximum absorption of the dye was monitored periodically with a UV−vis spectrophotometer.

CP MAS ^{29}Si NMR. Cross-polarization (CP) magic angle spinning (MAS) ^{29}Si nuclear magnetic resonance (NMR) spectroscopy was performed on the solid SiO_2 xerogels using a Bruker Instruments Model MSL-200. For the CP spectra, a 5 ms contact time was applied, and for MAS, a spinning rate of 3.5 kHz was used.

3. Results and Discussion

FTIR Monitoring of Reaction Rates. To obtain films with high optical quality from multialkoxide precursors, it is important to incorporate the silylated dyes homogeneously within the matrix. Caging can be enhanced by increasing the degree of dye bonding to the matrix and minimizing the extent of dye−dye bonding. Dye−dye bonding in this context refers to the condensation of two silylated dyes to each other. The best way to control such a structure is to match the reaction rates of the different alkoxide species. The hydrolysis and condensation reaction schemes for a silicon alkoxide are described in eqs 1 and 2, where R represents an alkyl

$$\equiv Si-OR + H_2O \rightarrow \equiv Si-OH + ROH \quad (1)$$

$$\equiv Si-OH + \equiv Si-OH \rightarrow \equiv Si-O-Si\equiv + H_2O \quad (2)$$

group (e.g., $-CH_3$, $-CH_2CH_3$). Using FTIR spectroscopy, the hydrolysis reaction was monitored by following the decrease in H_2O content and increase in the alcohol (ROH) content in the solution as the reaction proceeds. Reactions were carried out under acidic conditions to maximize the hydrolysis reactions and to minimize the condensation reactions, which result in H_2O formation.

H_2O has three relevant absorptions at 1647 cm^{-1} (bending), 3504 cm^{-1} (stretch), and 3571 cm^{-1} (stretch), while the hydroxyl group in EtOH has one relevant absorption at 3474 cm^{-1} (stretch). The peaks were identified from reference solutions of H_2O and EtOH. The hydrolysis rate of TEOS was monitored by disappearance of the H_2O (bending) peak at 1647 cm^{-1}. The hydrolysis rate of the silylated dye, on the other hand, was monitored by the decrease in the 3571 cm^{-1} H_2O absorption, because other infrared absorptions of the silylated dye overlapped with the 1647 cm^{-1} H_2O absorption and because the 3475 cm^{-1} EtOH absorption overlapped with the 3504 cm^{-1} H_2O absorption. The IR spectra in Figure 5 illustrate the decrease in H_2O content during the hydrolysis of TEOS and of a silylated coumarin dye (derCoum). The hydrolysis rate of the silylated dyes was found to be much slower than that of TMOS. Under acidic conditions and with stoichiometric amounts of water, complete hydrolysis of TMOS takes place within a few minutes;[20,21] hence the hydrolysis rate of TMOS could not be easily monitored by the technique used in this study.

An ethoxy-functional alkoxide (TEOS) hydrolyzes and condenses much more slowly than a methoxy-functional alkoxide (TMOS) due to steric hindrance of the bulkier ethoxy group.[20] The hydrolysis rate of derCoum was even slower than that of TEOS (see Figure 6). Alkyl-substituted silanes such as methyltriethoxysilane (MTEOS) are known to hydrolyze much faster than TEOS under acidic conditions.[22,23] The alkyl group substitution increases the stability of the charged transition state, enhancing the kinetics of hydrolysis. The slower kinetics of hydrolysis of derCoum (which can be considered an alkyl-substituted triethoxysilane) are likely due to the large steric hindrance caused by the large alkyl group, which is composed of the urethane dye linkage and the dye (where "dye" refers to the

(20) Brinker, C.; Scherer, G. *Sol−Gel Science*; Academic Press: Boston, 1990.
(21) Schmidt, H., Kaiser, A., Rudolph, M., Lentz, A., Schmidt, H., Kaiser, A., Rudolph, M., Lentz, A., Eds.; John Wiley & Sons: New York, 1986; pp 87−93.
(22) Schmidt, H. *J. Non-Cryst. Solids* **1985**, *73*, 681−691.
(23) Schmidt, H.; Scholze, H.; Kaiser, A. *J. Non-Cryst. Solids* **1984**, *63*, 1−11.

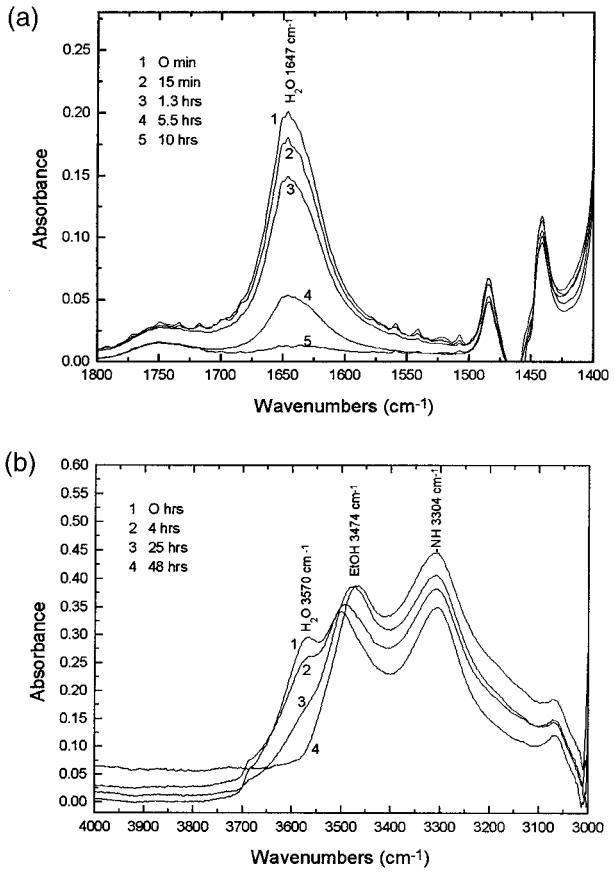

Figure 5. FTIR spectra of (a) TEOS and (b) derCoum at different hydrolysis times.

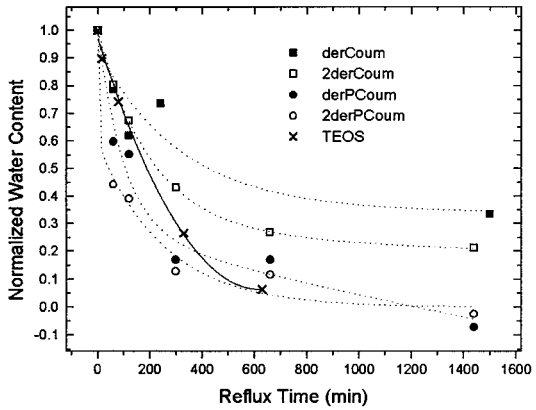

Figure 6. Water consumption as a function of reflux time for derCoum and TEOS in THF at 2.11 mol % under partial hydrolysis conditions.

"Coum" basic structure). Large alkyl groups in alkyl-substituted alkoxysilanes have been found to hydrolyze slower than smaller alkyl groups.[24,25] For example, Pohl et al.[24] found that a cyclohexane trialkoxysilane hydrolyzes 7 times slower than a methyltrialkoxysilane. Also, they reported a propyltrialkoxysilane to hydrolyze 2.6 times slower than a methyl trialkoxysilane.

To examine the steric hindrance effects in more detail, the lowest energy form of derCoum was determined by a molecular modeling program. It was found that derCoum curls up in its lowest energy state, such that the urethane linkage and the dye surround the triethoxysilane (Figure 7). The large blockage of the triethoxysilane group by the dye and the urethane linkage gives clear evidence that steric effects are likely causing the slower kinetics of hydrolysis of derCoum compared with TEOS.

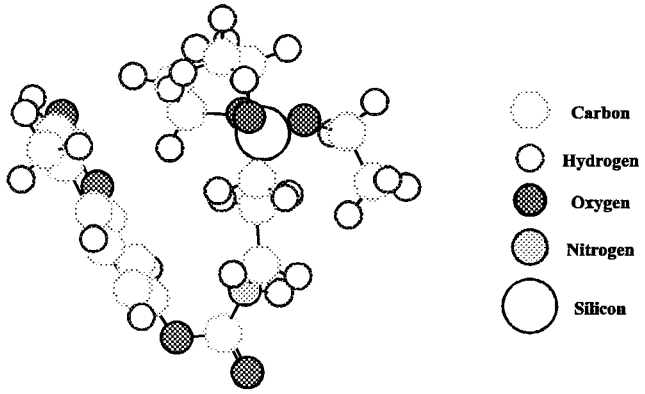

Figure 7. Ball-and-stick model of derCoum illustrating the lowest energy state of the dye.

The silylated dyes with the propyl linkage were found to hydrolyze faster than the urethane-linked dyes (Figure 6). The reason for this is not well understood. The derPCoum and the der2Pcoum dyes have a shorter link between the triethoxysilane groups and the coumarin moiety than the derCoum and 2derCoum molecules ($-CH_2CH_2CH_2-$ versus $-CH_2CH_2CH_2NHCO-$). The absence of the urethane linkage could give rise to low-energy states in which the triethoxysilane groups are less hindered by the coumarin part of the molecule. Also, the absence of the urethane linkage removes a group that would be competing for the hydrolysis agent through hydrogen bonding. For the same reasons (the competition between the effects of the stability of the charged transition state versus steric hindrance), TEOS hydrolyzed faster than the urethane-linked dyes but slower or equivalent to the propyl-linked dyes.

TMOS precursors were used for making the xerogel films (route 1) in the present study instead of TEOS due to ease and speed of processing. To match the reaction rates of the silylated dyes with that of TMOS, prehydrolysis of the silylated dyes was performed.

Dye Extraction. The degree of dye bonding to the inorganic matrix can be inferred from the dye extraction experiments. To prevent dye extraction from the host, the dye must be completely caged within the silica network (which is unlikely for most of the dye molecules) or the silylated dye must be covalently bound via at least one reactive group to the continuous matrix. The monofunctionalized dyes have three reactable sites, while the bifunctionalized dyes have six reactable sites. Therefore, other things being equal, the probability of getting bonding of the bifunctionalized dyes to the host matrix should be higher than with the monofunctionalized dyes. In a previous study, we reported the need for full hydrolysis conditions in order to prevent dye extraction from the host for a monofunctionalized coumarin dye, derCoum,[18] while under partial hydrolysis conditions the dye was extractable from the host. In the present work it was found that the bifunctionalized

(24) Pohl, E. *Kinetics and Mechanisms of Acid and Base-Catalyzed Hydrolysis of Alkyltrialkoxysilanes in Aqueous Solutions*; Pohl, E., Ed., 1983; p 4-B.

(25) Osterholtz, F.; Pohl, E. *J. Adhes. Sci. Technol.* **1992**, *6*, 127−149.

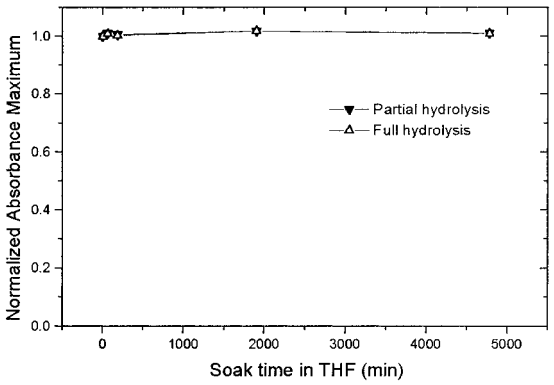

Figure 8. Dye extraction from a bifunctionalized dye 2der-Coum in xerogel films at $r = 0.10$ synthesized by route 1 under partial and full hydrolysis conditions.

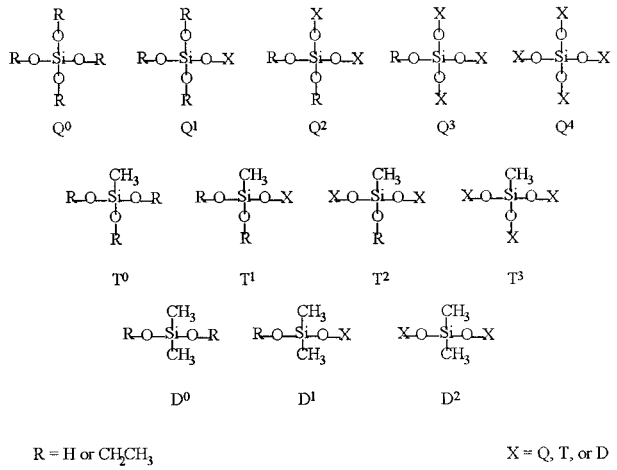

Figure 9. Possible silicate structures formed in the sol−gel process.[26]

dyes were not extractable from the host regardless of whether partial or full hydrolysis conditions were used (Figure 8). This reflects the ease of achieving dye bonding with bifunctionalized dyes.

Dye bonding to the matrix does not necessarily mean the dye is completely caged. The dye may be covalently bonded within the pores of the network where other species can easily diffuse to the dye and initiate photochemical interactions. It is likely that with full hydrolysis conditions a larger number of the six reactable sites have bonded to the silica matrix than with partial hydrolysis conditions. As the number of covalently bonded reactable sites increases, the probability of caging increases.

Solid-State ^{29}Si NMR. CP MAS solid-state ^{29}Si nuclear magnetic resonance (NMR) is a powerful technique for examining the structure of silicates.[26−30] Figure 9 illustrates possible silicate structures that can be formed by the sol−gel process. Q represents a quartenary oxygen tetrahedron; T represents a three

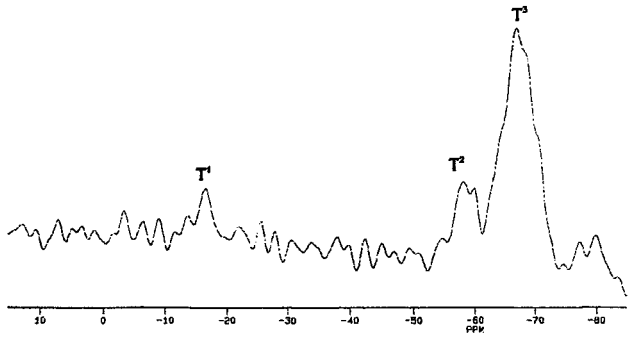

Figure 10. CP-MAS ^{29}Si NMR of a derCoum xerogel at $r = 0.10$ synthesized by route 1.

oxygen, one alkyl group tetrahedron; and D represents a two oxygen, two alkyl group tetrahedron. The superscripts denote the number of alkoxide groups that have reacted to form Si−O−Si linkages. Therefore, Q^0, T^0, and D^0 represent unreacted precursors, while Q^4, T^3, and D^2 represent completely reacted species.

NMR spectra for a derCoum xerogel will have T peaks from derCoum and Q peaks from TEOS. Quantitative evaluation of the T^0, T^1, T^2, and T^3 peaks characterizes the degree of dye bonding within the dye matrix. Cross-polarization (CP) and magic angle spinning (MAS) techniques were used to obtain enhanced signals and resolution with solid-state ^{29}Si NMR. Cross polarization enhances the intensity of Si atoms located near hydrogen atoms (<10 Å away).[31] The NMR spectrum for a derCoum xerogel prepared using 13 h of dye prehydrolysis is shown in Figure 10, and the results are summarized in Table 1.

The chemical shifts of the T and Q peaks were identified by their relative positions and by assigned peak values from previous solid-state ^{29}Si NMR work.[26,31,32] There was no identifiable evidence of any unreacted derCoum (T^0), indicating that all the dye has been bonded to the matrix. About 75% of the dye was fully condensed to the host as determined by the area of the T^3 peak, and about 25% of the dye was partially hydrolyzed as determined by area of the T^1 and T^2 peaks.

Dye caging is expected to increase with greater degree of condensation of the silylated dye. The probability of caging increases on going from T^0 species to the T^3 species. The T^0 dye molecules are not covalently attached to the silica matrix and is mobile to move to the pores of the matrix via the solvent. The T^1 dye molecules are more likely to be caged because it is covalently attached to the silica matrix, and further condensation of the host will likely surround the dye. By the same token, the T^2 (T^3) dye molecules are even more likely to be caged because they have two (three) linkages by which the silica matrix can grow around the dye. The amount of dye prehydrolysis time should affect the ratio between T^3:T^2:T^1. As the T^3 species increases, the probability of caging increases and so does the photostability. This concept is illustrated with proposed structures for Coum and derCoum xerogels shown in Figure 11. Coum in Figure 11a is not covalently attached to the matrix and is located in the

(26) Glaser, R.; Wilkes, G.; Bronnimann, C. *J. Non-Cryst. Solids* **1989**, *113*, 73−87.
(27) Lippmaa, E.; Magi, M.; Samoson, A.; Engelhardt, G.; Grimmer, A. *J. Am. Chem. Soc.* **1980**, *102*, 4889.
(28) Engelhardt, G.; Jancke, H.; Lippmaa, E.; Samoson, A. *J. Organomet. Chem.* **1981**, *210*, 295.
(29) Magi, M.; Lippmaa, E.; Somoson, A.; Engelhardt, G.; Grimmer, A. *J. Phys. Chem.* **1984**, *88*, 1518.
(30) Kim, J.; Plawsky, J.; Wagenen, E.; Korenowski, G. *Chem. Mater.* **1993**, *5*, 1118−1125.
(31) Klemperer, W.; Mainz, V.; Millar, D. *Mater. Res. Soc. Symp.* **1986**, *73*, 15−25.
(32) Babonneau, F. *New J. Chem.* **1993**, *18*, 1065−1071.

Table 1. Chemical Shifts (ppm) and the Fraction of Various Silicate Structures Measured by CP MAS ^{29}Si NMR for a DerCoum:SiO_2 Xerogel at $r = 0.10$

sample	T^0	T^1	T^2	T^3	Q^0	Q^1	Q^2	Q^3	Q^4
derCoum		−22	−54	−65.9			−93.7	−102.5	−111.0
xerogel	(0.00)	(0.08)	(0.17)	(0.75)	(0.00)	(0.00)	(0.05)	(0.69)	(0.26)
							(0.02)[a]	(0.42)[a]	(0.56)[a]

[a] Corrected ratio.

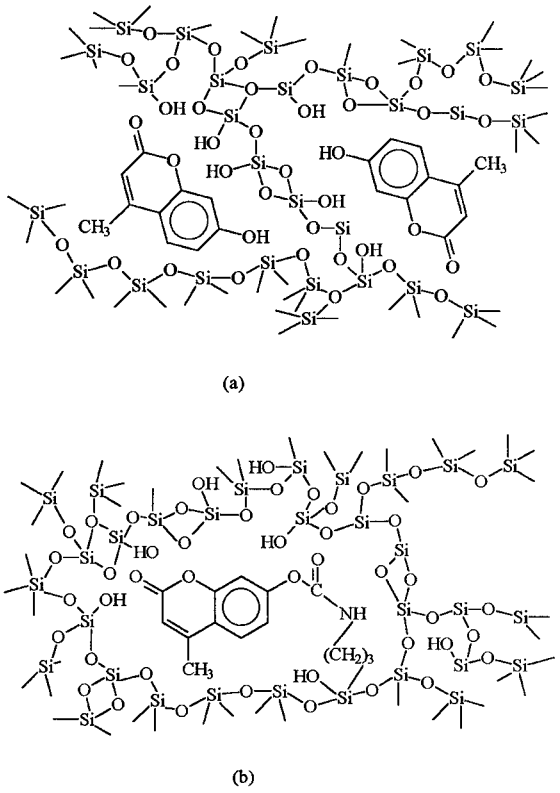

Figure 11. Proposed structures of (a) Coum and (b) derCoum in xerogel hosts.

open pores of the matrix, while derCoum (which is a T^2 species in this example) in Figure 11b is caged by the silica matrix.

Quantitative analysis of the Q species is a bit more complicated. The raw data from the CP technique reveal that the Q^2:Q^3:Q^4 ratios are 0.05:0.69:0.26. There is, however, a low cross-polarization efficiency with the Q^4 species because there are fewer H atoms nearby to facilitate the transfer of polarization. The Fourier transform (FT) NMR technique does not have this issue because all species are equally observed. Glaser et al.[26] found that the discrepancy was large between the CP and FT NMR techniques for a 100% TEOS-derived gel but was very small with PDMS:TEOS Polycerams. Hence corrections are needed for the xerogel samples; the corrected Q peaks are shown in Table 1. Corrections are based on a 100% TEOS derived sample (Glaser et al.[26]) with similar Q characteristics as the samples used in this study, where the correction factor is the ratio of the Q^n species measured by the FT technique to Q^n species measured by the CP technique. Such a correction was not needed with the T species, because hydrogen atoms are always near the Si in T species, because derCoum has hydrogen-containing alkyl groups directly bonded to Si.

Photostability. A typical fluorescence photostability curve measured by pumping with a N_2 laser for all the coumarin dye doped films is shown in Figure 12. Initially, the fluorescence intensity dropped rapidly but then decayed linearly over long times. This type of photostability behavior has also been observed in a number of other dye/solid host systems.[16,33−35] Since most samples showed no recoverability in fluorescence, both regimes represent permanent photodecay. Although a derCoum xerogel showed some recoverability, this represented only an 8% rise in fluorescence upon blocking the pump beam for 1 h after 23 000 pulses (see Figure 13). The initial decay has been attributed to dye molecules located in the open pores of the network, which are more prone to photodecay processes such as oxidation. This initial decay has been modeled and

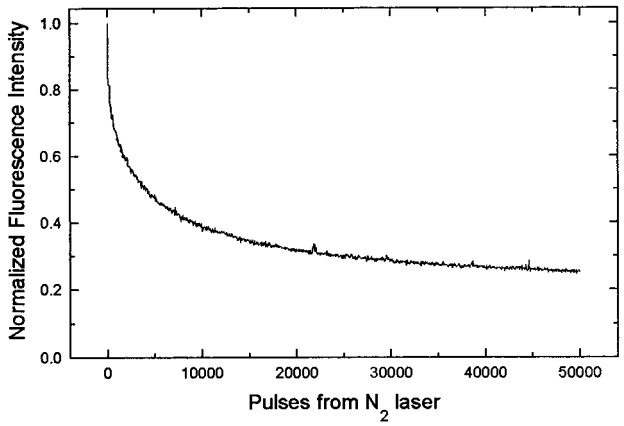

Figure 12. Typical fluorescence photostability curve of a coumarin xerogel at $r = 0.05$ synthesized by route 1.

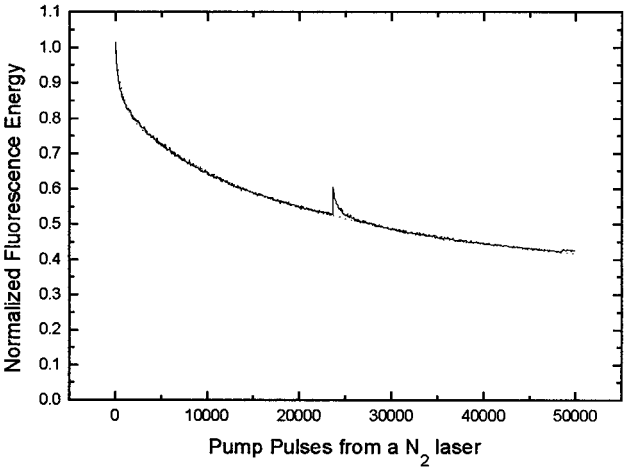

Figure 13. Photostability of a derCoum xerogel film synthesized by route 1 illustrating the partial reversibility of the initial decay in photostability.

(33) Knobbe, E.; Dunn, B.; Fuqua, P.; Nishida, F. *Appl. Opt.* **1990**, *29*, 2729−2733.
(34) Sastre, R.; Costela, A. *Adv. Mater.* **1995**, *7*, 198−202.
(35) Dunn, B.; Nishida, F.; Altman, J.; Stone, R. *Spectroscopy and Laser Behavior of Rhodamine-Dope Ormosils*; Dunn, B., Nishida, F., Altman, J., Stone, R., Eds.; 1992; pp 941−951.

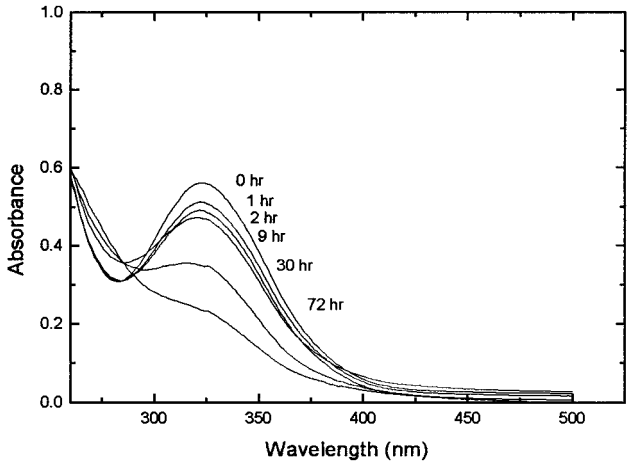

Figure 14. Absorption spectra of coumarin xerogel at $r = 0.05$ synthesized by route 1 upon exposure to UV light.

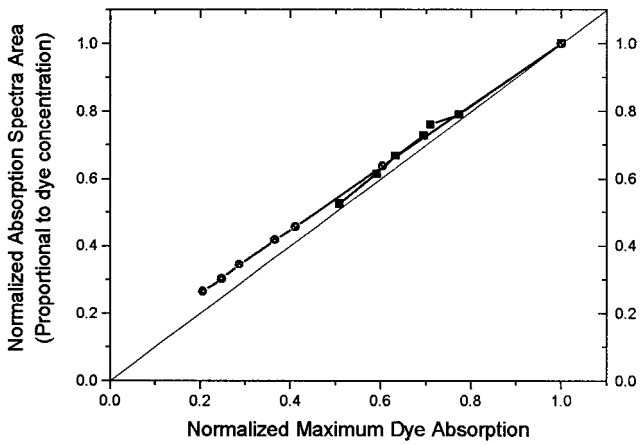

Figure 15. Normalized absorption spectra area as a function of the normalized maximum absorption of a derCoum xerogel at $r = 0.05$ synthesized by route 1.

discussed in greater detail elsewhere.[36,37]

To compare the samples quantitatively, a figure of merit (FOM) is defined to describe the rate of permanent dye degradation in the slow linear process. The FOM is defined as

$$\text{FOM} = m/b$$

where m is slope and b is the y intercept of the linear regression fit of the slow linear fluorescent decay. Dividing the slope by the y intercept provided normalized rates of fluorescence decay, and this allowed the comparison of samples with different fluorescence output intensities. The FOM values are negative, and a value of 0 would mean there is no decay in the fluorescent output in this region of time.

Photostability was also measured by pumping with a longwave UV lamp (>300 nm). UV photostability or absorption photostability monitors the absorbance of the dye as a function of UV lamp exposure time. Figure 14 illustrates the decay in the absorption spectra of a coumarin xerogel (route 1).

Most dye degradation processes result in the alteration or the destruction of the π-electron aromatic system, which results in the loss or the shifting of the absorption of the dye. The absorbance of the sample is linearly related to the concentration and is therefore a direct measure of the concentration. To compare accurately the dye degradation rate between samples, the samples for each experiment had the same dye concentration and sample thickness.

The absorption photostability measurements were typically carried out by measuring only the maximum absorbance of the dye. Figure 15 is a plot of the normalized area of the absorption spectra as a function of the normalized maximum in the absorption of the dye. The solid line represents a 1:1 correspondence between the two. Data from two different samples also show good 1:1 correspondence. The dye concentration is proportional to the area of the absorption spectra. Since the data show a good 1:1 correspondence, the drop in the maximum absorbance of the dye is also directly proportional to the dye concentration. Therefore, photostability data can be taken by simply monitoring the drop in the maximum absorbance of the dye, greatly simplifying the experimental procedure.

Effect of Prehydrolysis of the Dye. The FTIR spectroscopy studies of the reaction rates discussed earlier showed that the silylated dyes needed to be prehydrolyzed in order to increase the probability that they will be incorporated homogeneously within the host matrix. To improve photostability, the silylated dye must be caged within the matrix, and caging can be enhanced by increasing the degree of condensation of derCoum to the silica matrix. To explore this, various dye−xerogel films were coated from sol−gel solutions using different prehydrolysis times for the derCoum. Fluorescence photostability was measured, and the FOM was evaluated to determine the optimum prehydrolysis time.

Two different processing routes were explored. The first is the SiO_2 xerogel route 1 (described in the Experimental Section), where the prehydrolyzed dye solution was mixed with a prehydrolyzed TMOS solution to obtain the final xerogel solution. The second route is a variation of SiO_2 xerogel route 1, where the prehydrolyzed dye solution was mixed with TMOS, and then acidified water was added to hydrolyze the whole mixture.

The photostability results for the derCoum xerogel films as a function of prehydrolysis time of the dye are shown in Figure 16. Both processing routes showed a maximum in the photostability FOM for about 13 h of prehydrolysis. For the conditions explored here, the silylated dye hydrolyzed enough after 13 h such that the condensation rate of the dye and TMOS precursor closely match to maximize the dye−silica bonding, dye caging, and photostability. ^{29}Si NMR results (Table 1) confirm the large degree of dye bonding (i.e., large fraction of T^3 silicate species) for a derCoum xerogel sample processed with 13 h of prehydrolysis.

At short prehydrolysis times (<13 h), the lower photostability is attributed to the lack of dye caging by the network. Dye bonding to the host does not necessarily mean that the dye is caged. The dyes, which are bonded but not caged, are likely located within the pores

(36) Suratwala, T. *Photostability of Laser Dyes in Sol−Gel Derived Hosts*; Ph.D. Dissertation, University of Arizona: Tucson, 1996.
(37) Suratwala, T.; Davidson, K.; Gardlund, Z.; Uhlmann, D. R.; Bonilla, S.; Peyghambarian, N. *Solid State Lasers VI* **1997**, *SPIE 2986*, 141−152.

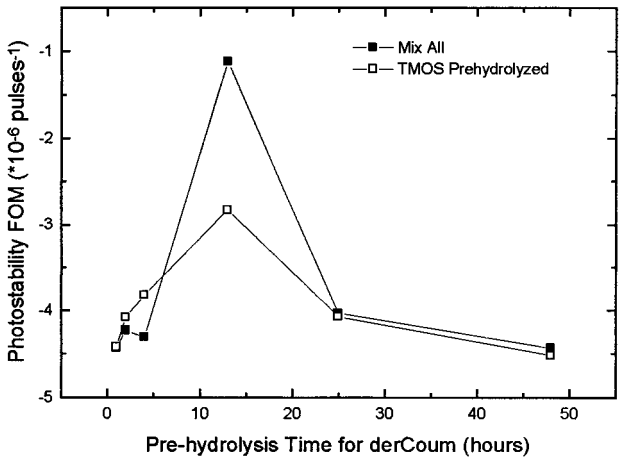

Figure 16. Photostability FOM of derCoum xerogel films at $r = 0.05$ synthesized by route 1 as a function of prehydrolysis time of the dye.

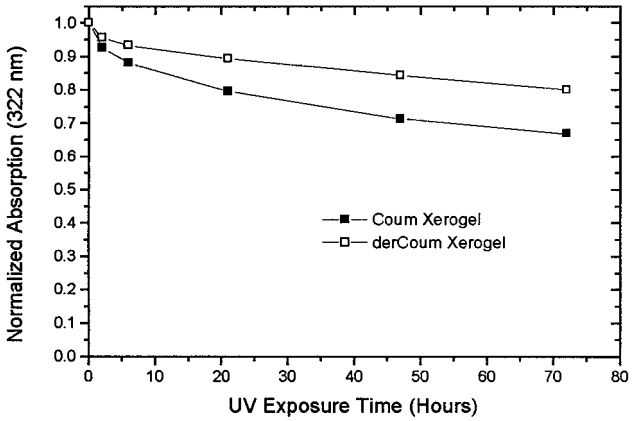

Figure 17. UV photostability of Coum and derCoum xerogel at 0.05 M synthesized by route 1.

Table 2. Photostability of Coumarin-Doped Xerogel Films at $r = 0.05$

dye	FOM (10^{-6} pulse^{-1})	normalized absorption after 72 h of UV exposure
Coum	−3.75	0.67
derCoum	−1.12	0.81
2derCoum	−5.64	0.35
derPCoum	−3.81	0.21
2derPCoum	−5.71	0.16

of the silica network. For long prehydrolysis times (>13 h), the dye has been hydrolyzed and a significant amount of self-condensation has occurred. This will lead to greater dye−dye bonding and less dye−silica bonding within the xerogel and hence decreased photostability. Greater dye−dye bonding should result in more dimerization reactions.

Xerogel Films. The photostability FOMs of all the dyes in SiO_2 xerogel hosts (route 1) are summarized in Table 2. The higher values of the FOMs (or the smaller absolute values of the FOMs) correspond to higher photostabilities. For comparison, the absorption photostabilities upon exposure to UV light are also summarized in the table; the absorption photostability is reported as the normalized absorption after 72 h of UV exposure (i.e., absorbance of the dye film after 72 h of UV lamp exposure divided by the absorbance of the dye film before exposure).

With optimized sol−gel processing conditions, a silylated dye SiO_2 xerogel film, derCoum (FOM= -1.12×10^{-6} pulse^{-1}), showed a 3-fold improvement in the photostability FOM compared to its unsilylated dye counterpart, Coum (FOM = -3.75×10^{-6} pulse^{-1}). The same photostability trend was observed with the absorption photostability (see Table 2 and Figure 17); after 72 h of UV exposure, the Coum xerogel film had only 33% of the dye degraded, while the derCoum had only 19% of the dye degraded.

By eliminating interaction of the dye molecules with other species, a number of dynamic processes are prevented (Figure 1). Because a great majority of the unsilylated dye is easily removed during solvent extraction, these dye molecules must be located within the open-pore network of the xerogel and are more likely to undergo photodecomposition through dynamic processes such as oxidation and dimerization. This type of reasoning correlates well to the observed improvement in photostability. Using a silylated laser dye provides improved photostability because the silylated dye has a greater tendency of being caged and immobilized within the host. Proposed structures for Coum and derCoum xerogels in Figure 11 illustrate the greater caging of derCoum.

There was not always a 1:1 correspondence between the two photostability methods. In other words, when the FOM was high for a particular dye xerogel, signifying a high photostability, the absorption photostability would not always signify the same trend in photostability. For example, the derPCoum xerogel had a FOM similar to that of Coum, but the absorption photostability of the derPCoum was much lower (see Table 2). The mechanism of dye degradation is likely different depending on the method of pumping. The UV lamp excitation is a continuous, broad band pump, while the N_2 laser pumping is pulsed and monochromatic. Thermal degradation is more likely with UV lamp pumping because it is continuous, not allowing the dye to return to the ground state or allowing for heat to dissipate. Another source of discrepancy between the two photostability measurements is that with the N_2 laser pumped photostability measurements, the calculated FOM is only a measure of the long-term decay; while with the absorption photostability measurements, it is a measure of the total decay.

The Coum SiO_2 xerogel and the monofunctionalized dye SiO_2 xerogels (derCoum, derPCoum) had a much higher fluorescence photostability than the bifunctionalized dye SiO_2 xerogels (2derCoum, 2derPCoum; see Table 2). These results seemingly contradict the earlier discussion of photostability. With dye bonding possible at six sites for the bifunctionalized dyes, the probability of dye caging is higher, which should lead to superior photostability compared with the monofunctionalized dyes. However, 2derCoum and 2derPCoum were synthesized from 5,7-dihydroxy-4-methylcoumarin (2Coum), while the monofunctionalized dyes were synthesized from Coum. The UV photodegradation of the silylated dyes and their unsilylated dye counterparts dissolved in MeOH at 10^{-4} M indicate that 2Coum is inherently less photostable than Coum (Figure 18). Hence the lower photostability of 2derCoum can be associated with the inherent lack of such stability of its unsilylated

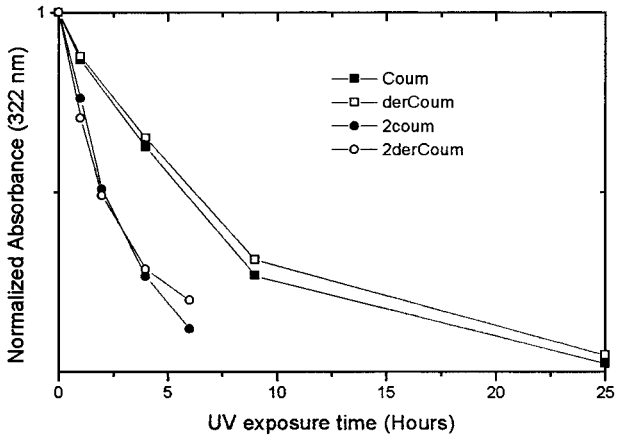

Figure 18. UV photostability of coumarin dyes in MeOH at 10^{-4} M measured in quartz cuvettes.

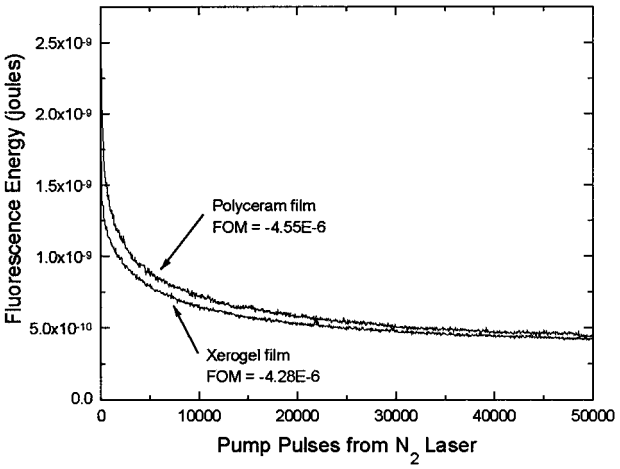

Figure 19. Fluorescence photostability of a derCoum xerogel synthesized by route 1 and a derCoum Polyceram synthesized by route 2 at $r = 0.10$.

precursor. The UV half-life of Coum was about 5.7 h, while for 2Coum it was only 2 h (Figure 18). The hydroxyl group substitution on the seven position makes the 2Coum more prone to photodegradation. Therefore, the FOMs of the monofunctionalized dyes and Coum cannot be compared to the FOMs of the bifunctionalized dyes because they are chemically derived from precursors with inherently different photostabilities.

Figure 18 also shows that the photostability of Coum and derCoum in MeOH were essentially identical. Therefore, silylation did not inherently change the photostability properties of the dye. These results indicate that the improved photostability observed with derCoum is associated with the dye/matrix interactions related to the dye caging within the xerogel host and not with the change in the inherent dye photostability upon silylation.

Polyceram Films. The fluorescence photostabilities of a derCoum SiO_2:PDMS Polyceram film (route 2) and a derCoum xerogel film (route 1) at the same dye concentration are shown in Figure 19. The photostability FOM was essentially the same for both samples. This suggests that the change in the host composition under the processing conditions explored here do not strongly influence the fluorescence photostability of coumarin dyes. SiO_2:PDMS Polycerams are attractive hosts because of the ease with which they may be

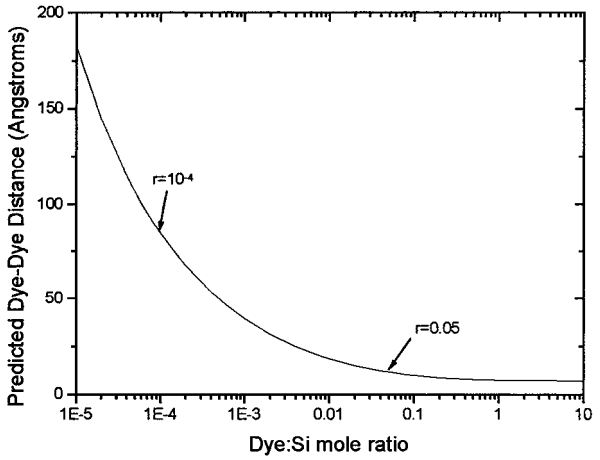

Figure 20. Predicted dye−dye distances as function of dye:Si mole ratio.

synthesized into monoliths compared to xerogel hosts.

In a concurrent study reported elsewhere,[38] the same coumarin dyes were incorporated within SiO_2:poly(dimethylsiloxane) (PDMS) Polyceram monoliths at $r = 10^{-4}$. Quantitative comparison of the photostability FOM of the Polyceram samples with the xerogels films was not possible because of the differences in dye concentration, sample thickness, and pump conditions. The FOM for the Polyceram monoliths were -4.69×10^{-6} pulse^{-1} with Coum, -2.64×10^{-6} pulse^{-1} with derCoum, -3.25×10^{-6} pulse^{-1} with derPCoum, -5.64×10^{-6} pulse^{-1} with 2derCoum, and -5.71×10^{-6} pulse^{-1} with 2derPCoum. Similar trends in photostability were observed as with the xerogels, e.g., derCoum Polycerams had improved photostability compared to the Coum Polyceram, and the bifunctionalized dye Polycerams had poorer photostability than the other coumarin dye Polycerams. One interesting difference is that the silylated dyes showed greater improvement in photostability in the Polyceram monoliths than in xerogel films. DerPCoum illustrates this point well. In a xerogel host, the FOM of derPCoum is similar to that of Coum, showing little improvement in photostability (see Table 2). In a Polyceram monolith, by contrast, a significant improvement in the photostability was observed.

This effect is likely caused by the difference in dye concentration; in the xerogel film the dye:Si mole ratio was $r = 0.05$, while in the Polyceram monolith it was $r = 10^{-4}$. The dye−dye distances within a sol−gel host were calculated for various dye concentrations assuming 100% reaction of the Si precursors and using 2.05 g/cm^2 as skeletal density of SiO_2 (Figure 20). At $r = 10^{-4}$ the average dye−dye distance is ≈85 Å, while at $r = 0.05$ it is ≈12 Å. Coum itself is 8 Å long, and silylated coumarins are much larger. At high dye concentrations, dye−dye interactions (e.g., dimerization) are likely for all the dyes (whether silylated or unsilylated); and this should result in a smaller improvement in photostability caused by the use of a silylated dye. At low dye concentrations, the silylated dye has a greater probability of being caged because the dye can bond at three

(38) Suratwala, T.; Gardlund, Z.; Davidson, K.; Uhlmann, D. R.; Bonilla, S.; Peyghambarian, N. *J. Sol−Gel Sci. Technol.* **1997**, *8*, 973−978.

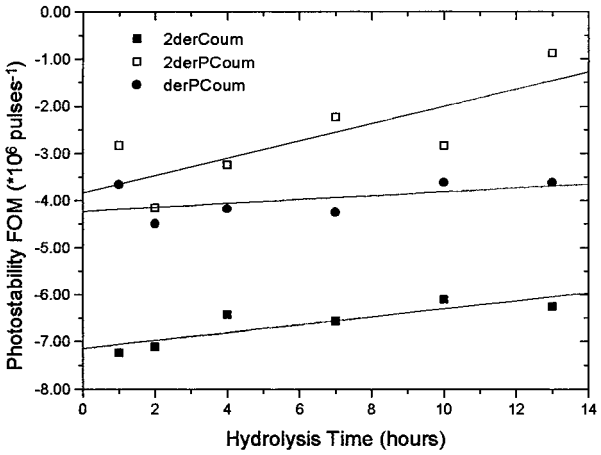

Figure 21. Effect of silylated dye hydrolysis time on the FOM of photostability for neat films synthesized by route 2.

sites for the monofunctionalized dyes (six sites for the bifunctionalized dyes) to initiate the caging and because there are more silicate species present to surround the dye, resulting in a greater improvement in photostability with respect to the unsilylated dye.

Neat Films. Neat films were synthesized by carrying out the hydrolysis/condensation reactions on a neat silylated coumarin precursor as described by route 3. Optically transparent films were obtained with all neat silylated coumarin dye films. The neat films have a high dye concentration. The dye:Si mole ratio for the monofunctionalized dyes is $r = 1.0$, and the mole ratio for the bifunctionalized dyes is $r = 0.5$. Xerogel films with the unsilylated dye at this concentration could not be obtained due to crystallization of Coum in the film. At such high concentrations with the neat films containing the functionalized dyes, dye−dye interactions are expected to be high (Figure 20). The relative fluorescence efficiencies (fluorescence output intensity/absorbance of film) of the neat films were typically 3−5 times lower than those of the same dyes within xerogel films at $r = 0.05$. This indicates that a large amount of fluorescence quenching is occurring in the neat films. Despite the low fluorescence efficiencies of the neat films, these films showed higher absolute fluorescence output than the xerogel films due to the greater number of fluorescing species per unit volume.

The photostability FOMs of the neat films could not be compared directly with those of xerogel samples due to the differences in concentration. It was observed, however, that the FOMs of the neat films increase with hydrolysis time for each of the silylated dyes (Figure 21). The improvement in photostability is attributed to the increase in the degree of cross-linking within the system with hydrolysis time. For the neat samples, the degree of cross-linking is the same as the degree of dye bonding. A greater increase in the FOM as a function of hydrolysis time was observed with the bifunctionalized dyes (2derPCoum and 2derCoum) than with the monofunctionalized dye (derPCoum). Because the bifunctionalized dyes have six bonding sites vs the three bonding sites of the monofunctionalized dye, the amount of caging possible is greater for the bifunctionalized.

Table 3. Photostability Results for Neat Coumarin Films

neat film	FOM (10^{-6} pulse^{-1})	normalized absorption after 72 h of UV exposure
derCoum		
derPCoum	−0.879	0.15
2derCoum	−3.62	0.27
2derPCoum	−6.25	0.22

Although a high FOM of -0.879×10^{-6} pulse^{-1} was obtained for the neat 2derPCoum film processed with 13 h of hydrolysis, poor photostability was observed by UV degradation of this sample (Table 3). Only 15% of the dye remained after 72 h of UV excitation. The cause of this is attributed to the difference in pumping. The UV lamp pumping was continuous and broad band, which would result in more sample heating than the nanosecond pulses from the N_2 laser. The neat samples are likely more prone to thermal degradation and also have lower thermal conductivity due to the large volume fraction of organic within the film.

4. Conclusions

Using sol−gel processing, a variety of synthesized coumarin laser dyes have been covalently attached within xerogel and Polyceram hosts. Their photostability properties were examined in detail and were found to vary with sol−gel processing conditions (namely, dye prehydrolysis time), dye composition and degree of functionalization, dye concentration, and method of optical pumping. Improvement in photostability was observed when the coumarin dyes were covalently attached to the host which is attributed to the greater probability of the dye to be caged than its unsilylated counterpart. The caged dye is less likely to interact with impurities (such as oxygen and other dye molecules) to undergo photodegradation.

Acknowledgment. The financial support of the Air Force Office of Scientific Research and the Corning Foundation Fellowship is gratefully acknowledged.

CM970340S